THE JOURNAL OF PHYSICAL CHEMISTRY LETTERS
A JOURNAL OF THE AMERICAN CHEMICAL SOCIETY

pubs.acs.org/JPCL Letter

Photodetachment and Tunneling Dissociation of Cryogenic Double-Rydberg Anions NH_4^-

Rui Zhang, Jiayi Chen, Shuaiting Yan, Wenru Jie, and Chuangang Ning*

Cite This: *J. Phys. Chem. Lett.* 2024, 15, 5612−5617 Read Online

ABSTRACT: The Rydberg radical NH_4 and the double Rydberg anion (DRA) NH_4^- have long aroused researchers' interests due to their potential for exploring the reaction dynamics of the $H + NH_3 \rightarrow H_2 + NH_2$ reaction, a prototypical penta-atomic system. In this study, we present high-resolution photodetachment spectroscopy of DRA NH_4^- and ion−molecule complex $H^-(NH_3)$. We observed multiple new photodetachment channels of DRA NH_4^-. The energy level of the excited state ($3p\ ^2T_2$) of the Rydberg radical NH_4 was determined to be 15052(94) cm^{-1}, in excellent agreement with the principal Schüler band (15061.61 cm^{-1}). Additionally, we observed the tunneling dissociation of NH_4^- in a cryogenic ion trap with its dissociation lifetime determined to be 19(2) ms.

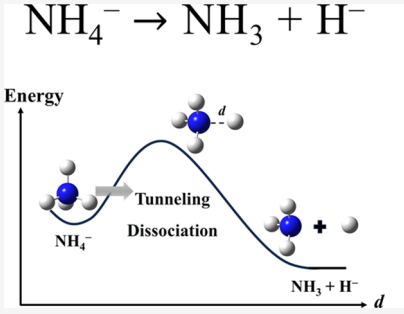

The concept of Rydberg molecules[1] was first introduced by Herzberg in 1981 through the emission spectra of the ammonium radicals NH_4,[2] wherein Rydberg states exhibit stability while their ground states are unstable, resembling H_3.[3] Subsequently, a neutralized ion-beam experiment[4] suggested the presence of a small barrier on their ground-state potential energy surface (PES), which separates the T_d symmetry minimum from the dissociative channel, with an evaluated lifetime <1 μs. Several theoretical studies[5−7] on NH_4 also support this conclusion, suggesting that the fragile Rydberg species readily overcome the shallow barrier and then dissociate into reactive radicals (i.e., $NH_4 \rightarrow H + NH_3$). Recently, anion photoelectron-photofragment coincidence (PPC) experiments combined with quantum dynamics calculations on a global PES by Hu et al.[8] indicate the dissociation of the nascent Rydberg radical NH_4 into H and NH_3 with a barrier energy of 0.329 eV, re-estimating this dissociation lifetime to be <100 ns.

While it is possible to probe the tunneling process of neutral metastable NH_4 species via the photodetachment of the double Rydberg anion (DRA) NH_4^-, experimental observation of the dissociation of the DRA has not been reported. NH_4^- was the first observed DRA molecule by Bowen and co-workers,[9−11] comprising a closed-shell parent cation core NH_4^+ and a pair of diffuse outer electrons. Both neutral NH_4 and NH_4^- DRA possess tetrahedral geometries that resemble the corresponding cation cores NH_4^+. The Bowen group studied NH_4^- DRA using photoelectron spectroscopy, and they also observed a separated feature contributed by the ion−molecule complex $H^-(NH_3)$ in the same energy spectrum. These two anionic isomers are distinguished on the energy spectrum by a sharp peak with a measured binding energy of 0.48 eV and a structureless broad peak at 1.11 eV, respectively. The photodetachment of the two anionic isomers provides a unique approach to probe the reaction dynamics of the $H + NH_3 \rightarrow H_2 + NH_2$ reaction, a prototypical penta-atomic system.[12−14] The latest measurements by the Continetti group reported 1.12(7) eV for $H^-(NH_3)$ and 0.48(6) eV for NH_4^- based on the fast anion beam PPC spectrometer.[8] So far, NH_4^- DRA has never been produced alone and is always accompanied by its $H^-(NH_3)$ isomer in the energy spectrum. On the theoretical side, high-level calculations have offered a solid complementary support for the identification of these anionic isomers.[15−18] $H^-(NH_3)$ located at the global minimum and NH_4^- located at a local minimum on the PES. In the present work, we report the high-resolution photoelectron spectra of two anionic isomers and the observation of the tunneling dissociation of NH_4^- DRA in a cryogenic ion trap.

Another motivation of the present work is to observe the Schüler band of NH_4 using high-resolution photodetachment spectroscopy at higher photon energy. In hollow-cathode discharges through NH_3, Schuster in 1872[19] and Schüler et al. in 1955[20] observed a number of emission bands. These diffuse bands remained a mystery for over a hundred years until the isotope studies conducted by Herzberg in 1981.[2] Initially, the two bands in the visible region were assigned to the ammonium radical NH_4 by Herzberg,[2,21] analogous to the D

Received: April 21, 2024
Revised: May 12, 2024
Accepted: May 15, 2024

https://doi.org/10.1021/acs.jpclett.4c01168
J. Phys. Chem. Lett. 2024, 15, 5612−5617

lines of the isoelectronic Na atom. However, precise assignments of the bands to the transitions of NH_4 were challenging at that time. In 1986, Watson et al. argued that the previous identification by Herzberg was not definitive.[22] They reassigned the Schuster bands to the reaction gases NH_3 and ND_3,[22] and the Schüler bands to the transition $^2T_2$ (3p) → $^2A_1$ (3s) of NH_4 instead of the proposed $^2E_1$ (3d) → $^2T_2$ (3p) assignment.[23] Theoretical calculations by Martin et al.[24] and Ortiz et al.[25] also supported their conclusions. Recently, the Continetti group[26] produced exotic neutral NH_4 by the charge exchange neutralization of the ammonium cation NH_4^+ and observed that the spacing between the assigned 3s ($\nu = 0$) peak and the highest-energy resolved feature ($3p_{max}$) is 1.87 eV (~15083 cm^{-1}) in the kinetic-energy-release (KER) spectrum, closely matching the principal Schüler band (15061.61 cm^{-1}).[21]

The experiments were conducted on our slow-electron velocity-map imaging apparatus equipped with a cryogenic ion trap (cryo-SEVI), with further details provided elsewhere.[27,28] In this study, both NH_4^- and $H^-(NH_3)$ were generated by expanding a mixed gas of ammonia and helium through a pulsed valve fitted with a high-voltage electron-gun ion source.[29] The backing pressure was about 5×10^5 Pa. The produced anions were guided into a radiofrequency (rf) octupole ion trap[30] with the assistance of the rf hexapole guide. The temperature of the ion trap could be adjusted from 300 to 5 K as it is mounted on the cold head of a liquid helium chiller. The trapped anions were cooled by collisions with the buffer gas composed of 20% H_2 and 80% He for a duration of 5−45 ms during the storage period. Subsequently, the anions can be extracted from the trap and mass-selected using time-of-flight (TOF).[31] In the photodetachment region, the selected NH_4^- or $H^-(NH_3)$ anions were photodetached at various photon energies by using a tunable optical-parametric-oscillator (OPO) laser. The detached photoelectrons were analyzed via a velocity-map imaging (VMI) spectrometer[32,33] and their distributions were reconstructed from the projected photoelectron image utilizing the maximum entropy velocity Legendre reconstruction (MEVELER) method.[34]

Figure 1 displays the full photoelectron energy spectrum of anionic isomers NH_4^- and $H^-(NH_3)$ acquired by using the cryo-SEVI method. The ion-source gas is a mixture of NH_3 and He in a ratio of ~1:2. Peak **a** is attributed to the photodetachment from the ground state NH_4^- to its neutral ground NH_4 (3s $^2A_1$). Both the anionic and neutral ammonia radicals have similar tetrahedral molecular geometries, which undergo barely any change during the photodetachment process, resulting in peak **a** appearing as a sharp atomic line. The binding energy of this vertical transition is the electron affinity of NH_4, determined to be 3833(43) cm^{-1} or 0.475(5) eV, consistent with the previous experimental findings by the Continetti group (0.48 ± 0.06 eV)[8] and the Bowen group (0.48 eV),[11] as well as with the newest theoretical result by Ortiz group (0.477 eV).[18] Peak **c**, with a measured binding energy of 9079(578) cm^{-1} or 1.12(7) eV, is associated with the $H^-(NH_3)$ complex. This measured value is also in close agreement with the predicted value by the Ortiz group (1.079 eV)[18] and the experimental value by the Bowen group (1.11 ± 0.01 eV).[11] Considering that the equilibrium geometry of $H^-(NH_3)$ corresponds to the pure repulsive region of its neutral PES, peak **c** appears broad and structureless due to the rapid dissociation dynamics. The weak peak **b** exhibits photon-energy dependence, observed at 460 and 515 nm but not at

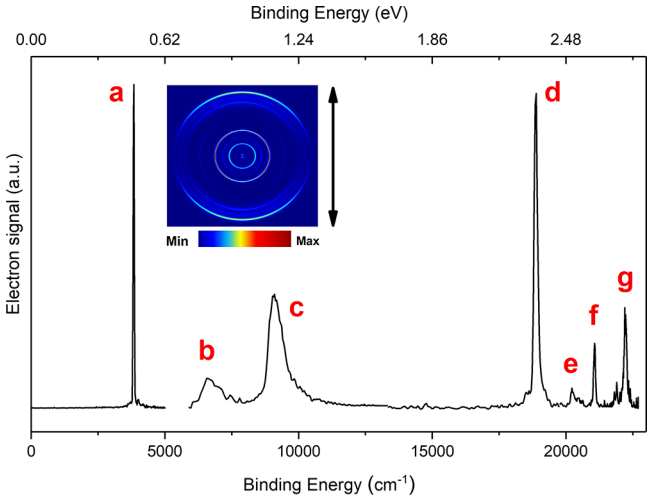

Figure 1. Full cryo-SEVI spectra of NH_4^- and $H^-(NH_3)$. The photoelectron image is obtained at 460 nm. The double-headed arrow indicates the polarization of the detachment laser. Peaks **d**−**g** are observed for the first time in the current work.

700 nm, as shown in Figure 2a. This observation is consistent with that observed by the Bowen group at 488 nm[11] but the Continetti group did not observe it at 775 nm.[8] This phenomenon might be due to a shape resonance during the photodetachment, analogous to observations in Na^-[35] and Cs^-.[36] Peak **b** arises from excitation of a vibrational mode during the resonant photodetachment, with a determined binding energy of 6743(728) cm^{-1} or 0.84(9) eV. The energy difference between peak **b** and peak **a** is 2910(729) cm^{-1}, closely matching the calculated vibrational frequency of the symmetric stretching mode of NH_4 by the Ortiz group (3109 cm^{-1})[37] and the Guo group (3032 cm^{-1}).[12] Thus, the final state of peak **b** is assigned to the symmetric stretching vibration mode (ν_1, A_1) of neutral NH_4.

A series of sharp peaks labeled as **d**−**g** appear in the photoelectron spectra at higher photon energies, which have not been observed before. During the experiment, we found that the relative intensity of peak **c** to other peaks changed when varying the trap time, as shown in Figure 2b. To determine which anionic isomer peaks **d**−**g** belong to, the relative intensity ratio of each peak at 45 ms to 5 ms is plotted in the Figure 2c. All spectra are normalized using peak **a** to compensate for the fluctuation of the ion beam intensity. For peaks from the same initial state of anions, their relative intensity should change uniformly versus the storage time in the ion trap.[28,38] Since the relative ratios of peaks **b** and **d**−**g** are consistent with that of peak **a** at 460 nm and peaks **f**−**g** are consistent with peak **d** at 440 nm, peaks **a**, **b**, and **d**−**g** are all from the same anionic ground state of NH_4^-. The energy difference between peaks **a** and **d** is measured to be 15052(94) cm^{-1}, or 1.866 (12) eV, which is in excellent agreement with the principal Schüler band (15061.61 cm^{-1}, $^2T_2$ (3p) → $^2A_1$ (3s) of neutral NH_4).[21] This indicates that peak **d** corresponds to the transition from the ground state of NH_4^- DRA to the first electronically excited state of NH_4. The theoretical result 1.749 eV by Ortiz et al.[25] also supports this identification. Another evidence is the distinct anisotropy parameter (β) of the photoelectron angular distribution (PAD), as the image in Figure 1 displays. β is 1.74 for peak **a** while it is −0.42 for peak **d** at the wavelength 460 nm. For NH_4^-, the outermost electron occupies the diffuse $2a_1$ orbital, similar to the 3s orbital of Na^-.

https://doi.org/10.1021/acs.jpclett.4c01168
J. Phys. Chem. Lett. 2024, 15, 5612−5617

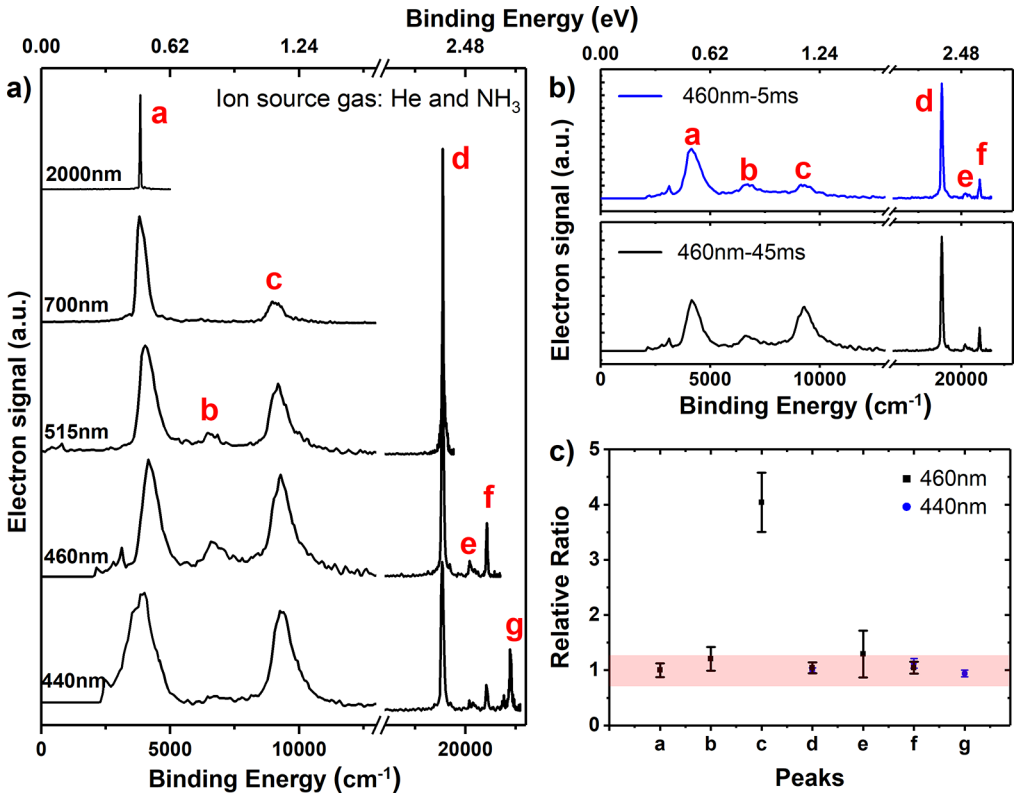

Figure 2. a) Photoelectron spectra of NH_4^- and $H^-(NH_3)$ acquired at various photon energies. b) Comparison of photoelectron spectra obtained with the storage time 5 ms (blue) and 45 ms (black) in the cryogenic ion trap at 460 nm. c) Relative intensity ratio of each peak with a storage time of 45 ms to 5 ms. The spectra were normalized using peak **a**. The black squares indicate peaks **a**−**f** obtained at 460 nm, and the blue circles indicate peaks **d**, **f**, and **g** obtained at 440 nm.

Consequently, the detached electrons associated with peak **a** are expected to exhibit a p-wave and have a positive β value, whereas those related to peak **d** are anticipated to have a different value owing to the two-electron process: one 3s electron is photodetached with another 3s electron excited to 3p. Therefore, the outgoing photoelectron for peak **d** cannot be the p-wave.[39] Since the next Rydberg excited state (3d $^2T_2$) of NH_4 is 21514 cm^{-1} higher than its ground state,[25] peaks **e**−**g** are impossible from other Rydberg states. Instead, they are assigned to three vibrational modes of NH_4 in its excited state 3p $^2T_2$. The high-level calculation of the vibrational frequencies of NH_4 in its Rydberg excited state 3p $^2T_2$ is a nontrivial task. Since Rydberg NH_4 (3p $^2T_2$) has a compact core NH_4^+ and its vibrational frequencies would be similar to those of NH_4^+, we estimated them using the vibrational frequencies of NH_4^+. The vibrational frequencies are measured to be 1353(182), 2185(142), and 3355(196) cm^{-1}, respectively, according to the gap among peaks **d**−**g**. They are close to the calculated values for the umbrella mode (ν_4, T_2, 1494 cm^{-1}), the twisting mode (ν_2, E, 1740 cm^{-1}), and the stretching mode (ν_3, T_2, 3500 cm^{-1}) of NH_4^+ at the B2PLYPD3/aug-cc-pVTZ level. The binding energies of all observed peaks, including assignments and β values of PADs, are listed in Table 1.

To explain the different changing trends observed for two isomers in the cryogenic ion trap, we further conducted the experiment under varying conditions. Theoretical predictions suggest two possible reactions in the ion trap.[8,40] One involves the conversion from NH_4^- DRA to $H^-(NH_3)$ complex, while the other entails the dissociation of NH_4^- into H^- and NH_3. By carefully controlling the ion source parameters, we can

Table 1. Binding Energy, Anisotropy Parameter (β) of the Photoelectron Angular Distribution (PAD), Assignment of Observed Peaks, and Experimental/Theoretical Vibrational Frequencies of the Neutral NH_4

Peak	Binding Energy (cm^{-1})[a]	β	Assignment	Vibrational Frequency (cm^{-1}) Experimental/Theoretical[b]
a	3833(43)	1.74	$NH_4^- \rightarrow NH_4$ (3s $^2A_1$)	
b	6743(728)	1.06	$NH_4^- \rightarrow$ (ν_1, A_1) of NH_4 (3s $^2A_1$)	2910/3032
c	9079(578)	1.33	$H^-(NH_3) \rightarrow H^*NH_3$	
d	18885(84)	−0.42	$NH_4^- \rightarrow NH_4$ (3p $^2T_2$)	
e	20238(161)	−0.42	$NH_4^- \rightarrow$ (ν_4, T_2) of NH_4 (3p $^2T_2$)	1353/1494
f	21070(115)	−0.14	$NH_4^- \rightarrow$ (ν_2, E) of NH_4 (3p $^2T_2$)	2185/1740
g	22240(177)	0.03	$NH_4^- \rightarrow$ (ν_3, T_2) of NH_4 (3p $^2T_2$)	3355/3500

[a]The value in the parentheses is the full width at the half-maximum (fwhm) of each peak. [b]The experimental results were obtained according to the energy gaps among the observed peaks. The theoretical value ν_1 = 3032 cm^{-1} for the ground NH_4 (3s $^2A_1$) is from ref 12, while the other values for the excited NH_4 (3p $^2T_2$) are calculated results in the present work.

https://doi.org/10.1021/acs.jpclett.4c01168
J. Phys. Chem. Lett. 2024, 15, 5612−5617

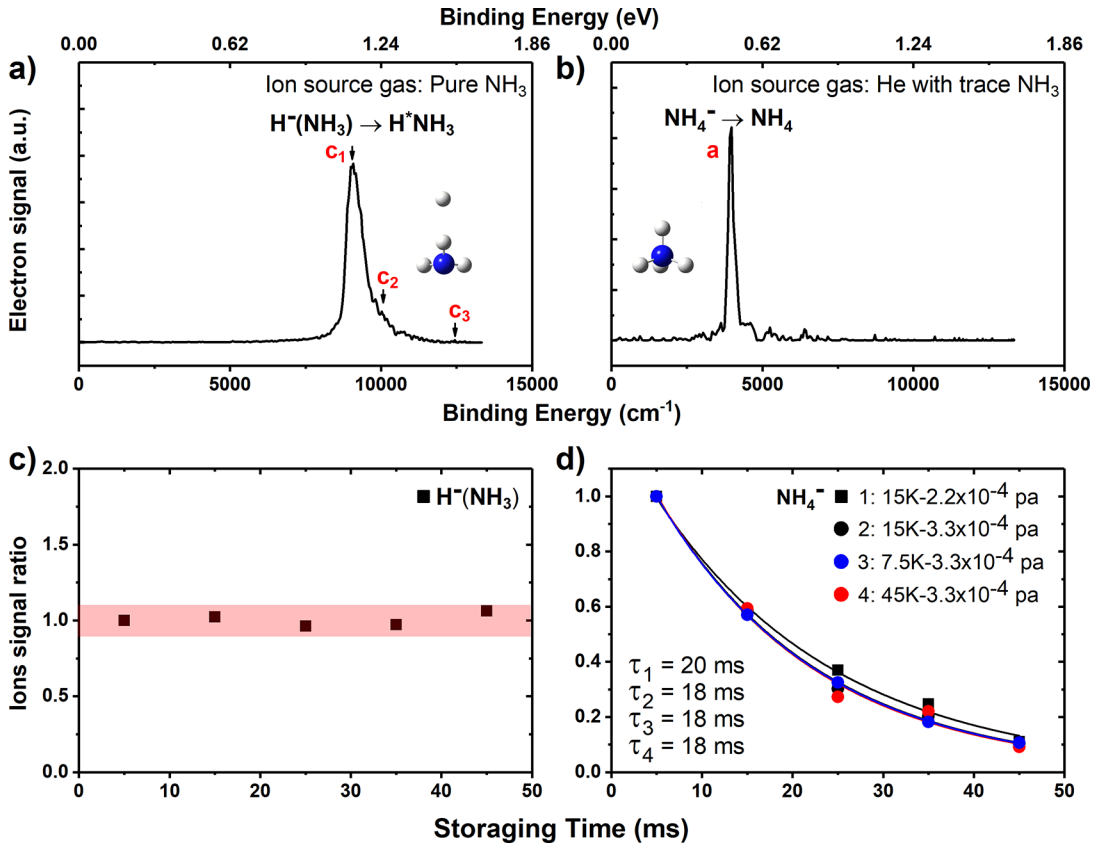

Figure 3. Photoelectron spectra of pure a) $H^-(NH_3)$ and b) NH_4^- at 750 nm. The black curve in panel a is in excellent agreement with the raw theoretical spectrum from ref 8. Tags c_1−c_3 denote the three predicted structures of $H^-(NH_3)$.[8] The geometric structures of $H^-(NH_3)$ and NH_4^- are depicted in each panel. c) Ion signal of $H^-(NH_3)$ as a function of the storage time in the ion trap. d) The ion signal of NH_4^- as a function of the storage time in the ion trap at different pressures and temperatures of the ion trap. The tunneling lifetime of NH_4^- was obtained via exponential fitting $I(t) = I_0e^{-t/\tau}$. The obtained values of τ are listed in the lower left corner.

generate pure $H^-(NH_3)$ and NH_4^- separately. When utilizing pure ammonia gas, only $H^-(NH_3)$ was produced, while a weaker signal of pure NH_4^- can be observed when using trace ammonia carried by helium, as shown in Figure 3a,b. Grumbling and Sanov[41] also acquired photoelectron spectra of $H^-(NH_3)$ alone using pure ammonia as the ion source gas. The pure NH_4^- alone has not been previously reported. The fact that these two anionic isomers could exist independently implies that NH_4^- DRA does not undergo transformation into the $H^-(NH_3)$ complex in the cryogenic ion trap.

The only remaining possible reaction pathway in the cryogenic ion trap is the dissociation of NH_4^- DRA. Following the confirmation that only $H^-(NH_3)$ exists in the cryogenic ion trap via the energy spectrum (Figure 3a), the ion intensity was recorded as the storage time ranged from 5 to 45 ms. As illustrated in Figure 3c, there is no observable change in the intensity of $H^-(NH_3)$. Furthermore, Figure 3a shows the high-resolution spectra of the $H^-(NH_3)$ complex, demonstrating excellent agreement with the high-level quantum dynamic simulations conducted by Hu et al.[8] Similarly, subsequent to confirming the exclusive presence of NH_4^- in the cryogenic ion trap based on the energy spectrum (Figure 3b), we observed an exponential decrease in the ion intensity of NH_4^- relative to the storage time, as shown in Figure 3d. To evaluate the possible collision or reaction effects caused by buffer gas (80% He + 20% H_2) in the ion trap, we varied the density of the buffer gas and the temperature of the ion trap. However, no notable change in the decay trend was observed, as shown in Figure 3d. The tunneling lifetime τ of NH_4^- into H^- and NH_3 was determined through exponential fitting to $I(t) = I_0e^{-t/\tau}$, where I represents the intensity of NH_4^- and t denotes the storage time of NH_4^- in the ion trap. The statistical average value of τ was found to be 19(2) ms. Notably, the tunneling lifetime of NH_4^- is much longer than that of the neutral NH_4.[8] To better understand this observation, we calculated the potential energy curve of NH_4^- dissociated into H^- and NH_3 along the C_{3v} pathway at the B2PLYPD3/aug-cc-pVTZ level, as shown in Figure 4. The barrier on the dissociation path is calculated as 1.09 eV relative to the energy of NH_4^- at equilibrium without the zero-energy correction, which is consistent with the previous theoretical results by Cardy et al. (0.8 eV),[42] Matsunaga et al. (1.4 eV),[17] and Melin et al. (0.7 eV).[43]

In conclusion, employing the cryo-SEVI method, we obtained high-resolution photoelectron spectra of double Rydberg anion NH_4^- and ion-complex $H^-(NH_3)$. The observed spectra exhibit excellent agreement with the previous quantum dynamics calculations. Additionally, several new peaks were observed, providing a solid support for assigning the Schüler band to the transition from the $^2T_2$ (3p) → $^2A_1$ (3s) of Rydberg radical NH_4. Furthermore, we observed the tunneling dissociation of NH_4^- in the cryogenic ion trap, estimating its lifetime as 19(2) ms. The study contributes to a deeper understanding of the exotic NH_4 and the reaction dynamics of $H + NH_3 \rightarrow H_2 + NH_2$.

https://doi.org/10.1021/acs.jpclett.4c01168
J. Phys. Chem. Lett. 2024, 15, 5612−5617

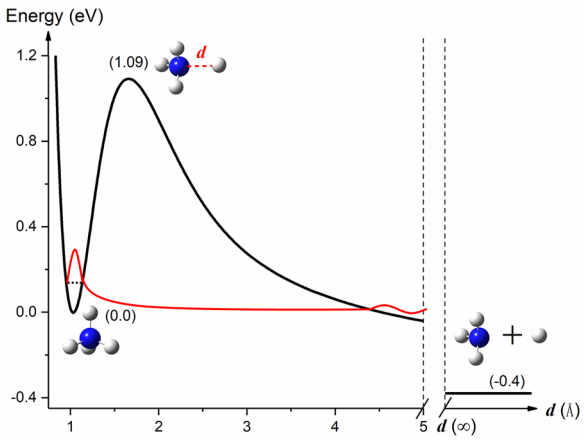

Figure 4. Calculated energy curve of dissociation of $NH_4^- \rightarrow H^- + NH_3$ along the C_{3v} dissociation pathway. The tunneling process is schematically represented by the red curve. *d* is the distance between the N and H atoms, as illustrated in the inset. NH_4^- at equilibrium is considered the reference point for energy. The asymptotic energy of H^- and NH_3 radicals is 0.4 eV lower than that of NH_4^-.[8]

AUTHOR INFORMATION

Corresponding Author

Chuangang Ning − *Department of Physics, State Key Laboratory of Low Dimensional Quantum Physics, Frontier Science Center for Quantum Information, Tsinghua University, Beijing 100084, China;* orcid.org/0000-0002-3158-1253; Email: ningcg@tsinghua.edu.cn

Authors

Rui Zhang − *Department of Physics, State Key Laboratory of Low Dimensional Quantum Physics, Frontier Science Center for Quantum Information, Tsinghua University, Beijing 100084, China;* orcid.org/0000-0001-9080-4528

Jiayi Chen − *Department of Physics, State Key Laboratory of Low Dimensional Quantum Physics, Frontier Science Center for Quantum Information, Tsinghua University, Beijing 100084, China*

Shuaiting Yan − *Department of Physics, State Key Laboratory of Low Dimensional Quantum Physics, Frontier Science Center for Quantum Information, Tsinghua University, Beijing 100084, China*

Wenru Jie − *Department of Physics, State Key Laboratory of Low Dimensional Quantum Physics, Frontier Science Center for Quantum Information, Tsinghua University, Beijing 100084, China*

Complete contact information is available at: https://pubs.acs.org/10.1021/acs.jpclett.4c01168

Notes

The authors declare no competing financial interest.

ACKNOWLEDGMENTS

This work is supported by the National Natural Science Foundation of China (NSFC) (Grant Nos. 12374244 and 12341401 to C.N.). S.Y. thanks the China Postdoctoral Science Foundation (Grant no. GZC20231367).

REFERENCES

(1) Herzberg, G. Rydberg molecules. *Annu. Rev. Phys. Chem.* **1987**, *38*, 27−56.

(2) Herzberg, G. Rydberg spectra of triatomic hydrogen and of the ammonium radical. *Faraday Discuss.* **1981**, *71*, 165−173.

(3) Herzberg, G. A spectrum of triatomic hydrogen. *J. Chem. Phys.* **1979**, *70*, 4806−4807.

(4) Gellene, G. I.; Cleary, D. A.; Porter, R. F. Stability of the ammonium and methylammonium radicals from neutralized ion-beam spectroscopy. *J. Chem. Phys.* **1982**, *77*, 3471−3477.

(5) Havriliak, S.; King, H. F. Rydberg radicals. 1. frozen-core model for rydberg levels of the ammonium radical. *J. Am. Chem. Soc.* **1983**, *105*, 4−12.

(6) Kassab, E.; Evleth, E. M. Theoretical study of the ammoniated NH_4 radical and related structures. *J. Am. Chem. Soc.* **1987**, *109*, 1653−1661.

(7) Cardy, H.; Liotard, D.; Dargelos, A.; Marinelli, F.; Roche, M. Ab initio CI study of the emission spectrum and the vibronic coupling in the $3p\ ^2T_2$ state of the ammonium radical. *Chem. Phys.* **1988**, *123*, 73−83.

(8) Hu, Q.; Song, H.; Johnson, C. J.; Li, J.; Guo, H.; Continetti, R. E. Imaging a multidimensional multichannel potential energy surface: photodetachment of $H^-(NH_3)$ and NH_4^-. *J. Chem. Phys.* **2016**, *144*, 244311.

(9) Coe, J. V.; Snodgrass, J. T.; Freidhoff, C. B.; McHugh, K. M.; Bowen, K. H. Negative ion photoelectron spectroscopy of the negative cluster ion $H^-(NH_3)_1$. *J. Chem. Phys.* **1985**, *83*, 3169−3170.

(10) Snodgrass, J. T.; Coe, J. V.; Freidhoff, C. B.; McHugh, K. M.; Bowen, K. H. Photodetachment spectroscopy of cluster anions. photoelectron spectroscopy of $H^-(NH_3)_1$, $H^-(NH_3)_2$ and the tetrahedral isomer of NH_4^-. *Faraday Discuss.* **1988**, *86*, 241−256.

(11) Xu, S.-J.; Nilles, J. M.; Hendricks, J. H.; Lyapustina, S. A.; Bowen, K. H., Jr. Double rydberg anions: Photoelectron spectroscopy of NH_4^-, $N_2H_7^-$, $N_3H_{10}^-$, $N_4H_{13}^-$, and $N_5H_{16}^-$. *J. Chem. Phys.* **2002**, *117*, 5742−5747.

(12) Li, J.; Guo, H. A nine-dimensional global potential energy surface for $NH_4(X^2A_1)$ and kinetics studies on the $H + NH_3 \leftrightarrow H_2 + NH_2$ reaction. *Phys. Chem. Chem. Phys.* **2014**, *16*, 6753−6763.

(13) Song, H.; Guo, H. Effects of reactant rotational excitations on $H_2 + NH_2 \rightarrow H + NH_3$ reactivity. *J. Chem. Phys.* **2014**, *141*, 244311.

(14) Song, H.; Li, J.; Yang, M.; Lu, Y.; Guo, H. Nine-dimensional quantum dynamics study of the $H_2 + NH_2 \rightarrow H + NH_3$ reaction: a rigorous test of the sudden vector projection model. *Phys. Chem. Chem. Phys.* **2014**, *16*, 17770−17776.

(15) Ortiz, J. V. Vertical and adiabatic ionization energies of NH_4^- isomers via electron propagator theory and many body perturbation theory calculations with large basis sets. *J. Chem. Phys.* **1987**, *87*, 3557−3562.

(16) Simons, J.; Gutowski, M. Double-rydberg molecular anions. *Chem. Rev.* **1991**, *91*, 669−677.

(17) Matsunaga, N.; Gordon, M. S. A theoretical study of NH_4^- and PH_4^-. *J. Phys. Chem.* **1995**, *99*, 12773−12780.

(18) Díaz-Tinoco, M.; Ortiz, J. V. Double rydberg anions with solvated ammonium kernels: electron binding energies and dyson orbitals. *J. Chem. Phys.* **2019**, *151*, 054301.

(19) Schuster, A. *Rep. Br. Assoc.* **1872**, *38*.

(20) Schüler, H.; Michel, A.; Grün, A. E. Über neue emissionsbanden bei elektrischer anregung des ammoniaks. *Z. Naturforsch. A* **1955**, *10*, 1−2.

(21) Herzberg, G. Spectra of the ammonium radical: the schüler bands. *J. Astrophys. Astron* **1984**, *5*, 131−138.

(22) Watson, J. K. G.; Majewski, W. A.; Glownia, J. H. Assignment of the schuster band of ammonia. *J. Mol. Spectrosc.* **1986**, *115*, 82−87.

(23) Watson, J. K. G. Assignment of the schüler band of the ammonium radical to the $3p\ ^2F_2$ - $3s\ ^2A_1$ electronic transition. *J. Mol. Spectrosc.* **1984**, *107*, 124−132.

(24) Martin, I.; Lavin, A. C.; Velasco, M.; Martin, M. O.; Karwowski, J.; Diercksen, G. H. F. Quantum defect orbital study of electronic

transitions in rydberg molecules: ammonium and fluoronium radicals. *Chem. Phys.* **1996**, *202*, 307−320.
(25) Ortiz, J. V.; Martın, I.; Velasco, A. M.; Lavın, C. Ground and excited states of NH_4: electron propagator and quantum defect analysis. *J. Chem. Phys.* **2004**, *120*, 7949−7954.
(26) Savee, J. D.; Mann, J. E.; Continetti, R. E. Stability of the ground and low-lying vibrational states of the ammonium radical. *J. Phys. Chem. Lett.* **2013**, *4*, 3683−3686.
(27) Tang, R.; Fu, X.; Ning, C. Accurate electron affinity of Ti and fine structures of its anions. *J. Chem. Phys.* **2018**, *149*, 134304.
(28) Zhang, R.; Lu, Y.; Tang, R.; Ning, C. Electron affinity of atomic scandium and yttrium and excited states of their negative ions. *J. Chem. Phys.* **2023**, *158*, 084303.
(29) Zhang, R.; Yan, S.; Song, H.; Guo, H.; Ning, C. Probing the activated complex of the F + NH_3 reaction via a dipole-bound state. *Nat. Commun.* **2024**, *15*, 3858.
(30) Ning, C.; Lu, Y. Electron affinities of atoms and structures of atomic negative ions. *J. Phys. Chem. Ref. Data* **2022**, *51*, 021502.
(31) Wiley, W. C.; McLaren, I. H. Time of flight mass spectrometer with improved resolution. *Rev. Sci. Instrum.* **1955**, *26*, 1150−1157.
(32) Eppink, A. T. J. B.; Parker, D. H. Velocity map imaging of ions and electrons using electrostatic lenses: application in photoelectron and photofragment ion imaging of molecular oxygen. *Rev. Sci. Instrum.* **1997**, *68*, 3477−3484.
(33) Yan, S.; Lu, Y.; Zhang, R.; Ning, C. Electron affinities in the periodic table and an example for As. *Chinese. J. Chem. Phys.* **2024**, *37*, 1−12.
(34) Dick, B. MELEXIR: maximum entropy Legendre expanded image reconstruction. a fast and efficient method for the analysis of velocity map imaging or photoelectron imaging data. *Phys. Chem. Chem. Phys.* **2019**, *21*, 19499−19512.
(35) Schulz, G. J. Resonances in electron impact on atoms. *Rev. Mod. Phys.* **1973**, *45*, 378−422.
(36) Scheer, M.; Thøgersen, J.; Bilodeau, R. C.; Brodie, C. A.; Haugen, H. K.; Andersen, H. H.; Kristensen, P.; Andersen, T. Experimental evidence that the $6s6p\,^3P_J$ states of Cs^- are shape resonances. *Phys. Rev. Lett.* **1998**, *80*, 684−687.
(37) Ortiz, J. V. A double rydberg anion with a hydrogen bond and a solvated double rydberg anion: interpretation of the photoelectron spectrum of $N_2H_7^-$. *J. Chem. Phys.* **2002**, *117*, 5748−5756.
(38) Lu, Y.; Tang, R.; Fu, X.; Ning, C. Measurement of the electron affinity of the lanthanum atom. *Phys. Rev. A* **2019**, *99*, 062507.
(39) Tang, R.; Fu, X.; Lu, Y.; Ning, C. Accurate electron affinity of Ga and fine structures of its anions. *J. Chem. Phys.* **2020**, *152*, 114303.
(40) Song, K.; Song, H.; Li, J. Validating experiments for the reaction H_2 + NH_2^- by dynamical calculations on an accurate full-dimensional potential energy surface. *Phys. Chem. Chem. Phys.* **2022**, *24*, 10160−10167.
(41) Grumbling, E. R.; Sanov, A. Solvation effects on angular distributions in $H^-(NH_3)_n$ and $NH_2^-(NH_3)_n$ photodetachment: Role of solute electronic structure. *J. Chem. Phys.* **2011**, *135*, 164301.
(42) Cardy, H.; Larrieu, C.; Dargelos, A. An ab initio study of the tetrahedral NH_4^- ion. *Chem. Phys. Lett.* **1986**, *131*, 507−512.
(43) Melin, J.; Ortiz, J. V. OH_3^- and $O_2H_5^-$ double rydberg anions: predictions and comparisons with NH_4^- and $N_2H_7^-$. *J. Chem. Phys.* **2007**, *127*, 014307.

https://doi.org/10.1021/acs.jpclett.4c01168
J. Phys. Chem. Lett. 2024, 15, 5612−5617